

## The effect of rock cover fraction on the retrieval of surface soil moisture at L-band

N. Ye<sup>1</sup>, J.P. Walker<sup>1</sup>, R. Panciera<sup>1</sup>, D. Ryu<sup>1</sup>, C. Rüdiger<sup>1</sup>, and R.J. Gurney<sup>2</sup>

<sup>1</sup>Department of Civil and Environmental Engineering, University of Melbourne, Australia

<sup>2</sup>NERC Environmental Systems Science Centre, University of Reading, United Kingdom

Email: [n.ye@civenv.unimelb.edu.au](mailto:n.ye@civenv.unimelb.edu.au)

**Abstract:** The Soil Moisture and Ocean Salinity (SMOS) mission, developed by the European Space Agency (ESA), will be launched in the second half of 2009. It will be the first L-band (~1.4 GHz) passive microwave satellite specifically designed for global soil moisture observations, with an expected accuracy for the retrieved soil moisture of ~0.04 m<sup>3</sup>/m<sup>3</sup>. While passive microwave observations have been widely acknowledged to give the most accurate information on soil moisture, these sensors are characterized by low spatial resolution footprints, being on the order of 50km. One of the key difficulties with observations at this scale is the heterogeneity that exists in land surface features. However, past and current soil moisture retrieval algorithms have typically assumed a homogeneous pixel approach. Thus, in order to maximize the soil moisture retrieval accuracy, the various land surface features that exist in a satellite footprint should be taken into account. While the SMOS retrieval algorithm distinguishes between three different surface types (bare soil, herbaceous and woody vegetation), at this stage it does not take into consideration other sub-pixel effects such as the brightness temperature contribution from open water bodies, rock cover or urban areas, which are expected to affect the overall soil moisture retrieval accuracy for many parts of the world. This study explores the impact of surface rock on the retrieval of surface soil moisture for short vegetation covered fields by comparing retrieved soil moisture estimates with and without accounting for the presence of rock in a synthetic framework. First, the microwave “observation” used to retrieve soil moisture is simulated by accounting for the contribution of rocks to the overall emission, assuming that rock behaves like very dry soil with a fixed dielectric constant and a smooth surface. The soil moisture is then retrieved using the homogeneous pixel approach. The simulation of microwave emission is based on a representative short grass field with various surface rock cover fractions, soil moisture contents and vegetation conditions. The results illustrate that rock induced soil moisture retrieval error is dependent on soil moisture and vegetation water content since the brightness temperature difference between soil and rock impacts the soil moisture retrieval error. The omission of rock cover from the retrieval algorithm leads to an overestimation of the bulk soil moisture content for low soil moisture conditions and an underestimation for high soil moisture conditions. Taking 30% rock cover fraction as an example, the maximum error in the bulk soil moisture estimation is as much as 0.04 m<sup>3</sup>/m<sup>3</sup> in bare soil and up to 0.10 m<sup>3</sup>/m<sup>3</sup> in wet soil covered by short grass vegetation. It should be noted however that these results may be highly dependent on two key assumptions of this paper; i) that rock can be modelled as a smooth surface, and ii) that there is no vegetation cover over the rock.

**Keywords:** passive microwave, soil moisture, remote sensing, rock fraction

## 1. INTRODUCTION

The Soil Moisture and Ocean Salinity (SMOS) mission, which will be the first dedicated soil moisture satellite, is currently scheduled for launch in the second half of 2009. SMOS consists of an L-band (~1.4 GHz) passive microwave sensor that will provide multi-angular observations in dual polarization using a new synthetic aperture technique (Kerr *et al.*, 2003). Passive microwave observations at L-band have been shown to be the most promising of the different remote sensing techniques for routine mapping of surface soil moisture at global scales, due to its ability to penetrate cloud, its direct relationship with soil moisture through the soil dielectric constant, and a reduced sensitivity to land surface roughness and vegetation cover (Jackson and Schmugge, 1989; Njoku *et al.*, 2002). While there have been a number of satellites operating at frequencies above 6 GHz (e.g. SMMR, AMSR-E, and WindSat), this is the first space-borne sensor to make long-term measurements at L-band.

Over the past three decades the quality of soil moisture retrieval from passive microwave remote sensing has been significantly improved. Moreover, Owe *et al.* (2008) have recently published a soil moisture product covering the years 1978-2007 using the available high frequency data from a series of satellites. While several of these recent soil moisture products show a good relationship with in-situ observations for areas of low vegetation cover (Rüdiger *et al.*, 2009), their retrieval error is typically above  $0.06 \text{ m}^3/\text{m}^3$ . Furthermore, all past soil moisture retrieval algorithms have been developed assuming a homogeneous land surface cover, with the exception of the SMOS algorithm (Kerr *et al.*, 2007), which allows for three different surface types within the satellite footprint. However, the influences of surface rock, water bodies, or urban centres within the sensor's field of view are not currently accounted for, and this will introduce a so far largely unquantified uncertainty in the soil moisture retrieval accuracy (Delwart *et al.*, 2008). This paper explores the first of these effects in a synthetic study in order to quantify this effect.

To date only a few experiments (e.g. Jackson *et al.*, 1992; Monerris *et al.*, 2008) have been conducted to examine the effect of rocks on soil radiometric emission at L-band. Those studies identified three main characteristics that affect the soil response: 1) rocks do not absorb any appreciable amount of water but they can occupy a large part of the soil space; 2) the low dielectric constant of rock reduces the average dielectric constant of the rock-soil mixture; and 3) the presence of rock may increase the surface roughness. The combined impact of these three effects is to alter the land surface emission in a complex way. Moreover, as rocks do not contribute to the soil moisture content, data collected with portable soil moisture probes during field campaigns will typically give an overestimation of the bulk soil moisture content, as the probes can only be inserted into soils having a relatively low rock fraction. While the effect of the surface rock fraction on the microwave emission from soil has been studied in relation to its emission characteristics (Jackson *et al.*, 1992; Monerris *et al.*, 2008), its effect on soil moisture retrieval accuracy has not yet been explored.

This study simulates the impact of rock on brightness temperature observation and the subsequent soil moisture retrieval, using the L-band Microwave Emission of the Biosphere (L-MEB; Wigneron *et al.*, 2001, 2007) model, which is the basis for the SMOS Level 2 retrieval algorithm. Consequently, the relationship of retrieved soil moisture to bulk soil moisture under the presence of surface rock is explored.

## 2. METHODOLOGY

The effect of rock fraction on soil moisture retrieval is studied here by comparing synthetic "truth" soil moisture with retrieved soil moisture from radiometric "observations" at L-band. The observations were synthetically generated by using the truth soil moisture and our current understanding of rock effects on microwave emission. Moreover, they were calculated for a range of rock cover fractions, vegetation conditions and soil moisture content. The rock cover effect on soil moisture was studied by subsequently retrieving the soil moisture without taking the surface rock fraction into consideration. The retrieved soil moisture was then compared with the original truth bulk moisture. Essentially, the test consists of the following three steps: 1) assigning parameters and ancillary data for the radio brightness model; 2) generating synthetic brightness temperature observations; and 3) retrieving soil moisture and vegetation water content simultaneously using the same parameters and ancillary data as used to derive the observations but without accounting for the presence of rock, as described in the following sections.

### 2.1. Land Surface Representation

A land surface representation was created to simulate the field conditions of varying rock fraction in various vegetation conditions ranging from bare soil to short grass. This land surface representation consists of a rock component without any overlying vegetation coverage and a soil component covered by short grass. Each component was assumed to be homogeneous and independent from each other, which means

**Table 1.** Land surface parameters used in the soil moisture retrieval algorithm (after Panciera *et al.*, 2009).

Sand Content $S$ (%)	67	Vegetation structure $tt_H$	1	Roughness $H_R$	0.5
Clay Content $C$ (%)	15	Vegetation structure $tt_V$	1	Roughness exponent $N_{RH}$	0
Bulk Density $\rho$ (g/cm <sup>3</sup> )	1.1	Scattering albedo $\omega_H$	0	Roughness exponent $N_{RV}$	0
Vegetation parameter $b$	0.15	Scattering albedo $\omega_V$	0.05		

surrounding vegetation has no attenuation impact on passive microwave emission from rock component. Moreover, the soil component was assumed to have soil, vegetation and roughness characteristics similar to those found at Roscommon farm in the Goulburn River Catchment (Panciera *et al.*, 2009). For all cases, the land surface was assumed to have no relief changes in order to remove any topographic effects on the soil moisture retrieval, and the rock component surface was assumed to be smooth. Consequently, the bulk moisture of the pixel is calculated by:

$$SM_{bulk} = (1 - f_r) \cdot SM_{soil}, \quad (1)$$

where  $f_r$  and  $SM_{soil}$  are the rock cover fraction and soil component moisture in the pixel, respectively.

## 2.2. Synthetic Brightness Temperature Generation

Eleven parameters (Table 1) were used to generate synthetic brightness temperature and subsequently invert soil moisture for each scenario, using L-MEB. For simplification purposes, the temperatures of rock, soil and vegetation were assumed to be identical and were set to 300 K. At the same time, the soil component moisture  $SM_{soil}$  was varied from 0.001 to 0.601 m<sup>3</sup>/m<sup>3</sup> in 0.001 m<sup>3</sup>/m<sup>3</sup> steps, and the Vegetation Water Content (VWC) values of soil component varied from 0.0 to 1.0 kg/m<sup>2</sup> in 0.02 kg/m<sup>2</sup> steps covering the whole range of VWC of short vegetation. This allowed the rock impact to be explored for a typical land surface under a range of soil moisture and vegetation conditions. The total brightness temperature of the land surface was assumed to be the sum of the brightness temperature derived from the two surface components weighted by its rock cover fraction:

$$TB_p = (1 - f_r) \cdot TB_{s,p} + f_r \cdot TB_{r,p}, \quad (2)$$

where  $TB$  is brightness temperature; subscripts  $p$ ,  $s$ , and  $r$  are the signal polarization ( $p$ , horizontal or vertical) for the soil ( $s$ ) and rock ( $r$ ) components.

In the ‘ $\tau$ - $\omega$  model’ (Mo *et al.*, 1982), the brightness temperature emission from the soil-vegetation layer is defined as the sum of three terms: 1) the upward vegetation emission scattered by the atmosphere, 2) the downward vegetation emission reflected by the soil and attenuated by the vegetation layer and then scattered by the atmosphere, and 3) the soil emission attenuated by the vegetation layer:

$$TB_{s,p} = (1 - \omega_p) \cdot (1 - \gamma_p) \cdot (1 + \gamma_p \Gamma_{s,p}) \cdot T_v + (1 - \Gamma_{s,p}) \cdot \gamma_p \cdot T_s, \quad (3)$$

where  $T_v$  and  $T_s$  are the effective vegetation and soil temperatures; and  $\omega_p$  and  $\gamma_p$  are the single scattering albedo and transmissivity of the vegetation layer. The reflectivity of a rough soil surface  $\Gamma_{s,p}$  is a function of the smooth soil surface reflectivity  $\Gamma_{s,p}^*$ , the incidence angle  $\vartheta$ , and the roughness parameters  $H_R$  and  $N_{Rp}$  (Wang and Choudhury, 1981; Wigneron *et al.*, 2001) given by:

$$\Gamma_{s,p} = \Gamma_{s,p}^* \cdot \exp[-H_R \cos^{N_{Rp}}(\vartheta)]. \quad (4)$$

The smooth surface reflectivity  $\Gamma_{s,p}^*$  is calculated through the Fresnel equations as a function of polarization  $p$ , relative dielectric constant of the soil  $\epsilon' + \epsilon''i$ , and the incidence angle  $\vartheta$ . Soil dielectric constant can be estimated from the soil component moisture  $SM_{soil}$  through the mixing model of Dobson *et al.* (1985). The transmissivity of the vegetation layer  $\gamma_p$  is determined by the vegetation optical depth at nadir  $\tau_{NAD}$  and the parameter  $tt_p$  that corrects the optical depth for non-nadir views at each polarization by:

$$\gamma_p = \exp[-\tau_{NAD} \cdot (tt_p \cdot \sin^2(\vartheta) + \cos^2(\vartheta)) \cdot \cos^{-1}(\vartheta)]. \quad (5)$$

According to Kerr *et al.* (2007) rocks can be assumed to behave like very dry soil, and their dielectric constant ranges from 2.4 to 9.6 at frequency of 400 MHz and 35 GHz (Ulaby *et al.* 1986). Ulaby *et al.* (1990) measured dielectric properties of 80 rock samples at frequency from 0.5 to 18 GHz in steps of 0.1 GHz for the real part. The results illustrate that real part of dielectric constant of rock ( $\epsilon'$ ) is independent of frequency, but has a correlation with the rock bulk density ( $\rho_b$ ) as:

$$\epsilon' = (1.96 \pm 0.14) \rho_b. \quad (6)$$

For the purpose of this study, it is assumed that rock behaves like a very dry bare soil with a smooth surface, and a temporally stable dielectric constant  $4.7 + 0.7i$ , which is the average value of dielectric constant measurement of rock samples at L-band in Jackson *et al.* (1992). Consequently the important assumptions here are that 1) the rock emission behaves like a smooth surface and 2) there is no vegetation layer over the rock. The radiometric emission from a rock surface can thus be calculated through:

$$TB_{r,p} = (1 - \Gamma_{r,p}) \cdot T_r, \tag{7}$$

where  $T_r$  is the rock surface temperature,  $\Gamma_{r,p}$  is the rock surface reflectivity calculated through Fresnel equations, assuming that the rock surface is smooth and horizontal that the incidence angle is equal to that for the soil surface. The sensitivity of soil moisture retrieval to the real part of rock dielectric constant, as well as to rock rough and rock temperature, is examined later.

### 2.3. Soil Moisture Retrieval

The surface soil moisture content was retrieved from the synthetically generated brightness temperature observations that accounted for the rock fraction, by using the L-MEB model without considering a rock cover fraction. The nonlinear optimisation scheme used for the retrieval is an iterative algorithm that optimises soil moisture and vegetation water content simultaneously. It aims to minimize the difference between the radiometric observation and the modelled brightness temperature. When the minimized difference exceeds the assigned tolerance, a non-convergence flag is returned.

The rock induced error is therefore the difference between the truth soil moisture and the surface soil moisture retrieved from the synthetic forward observation. A number of scenarios were simulated to identify the effect of the rock cover under varying conditions, by changing the rock cover fraction, surface soil moisture, incidence angle, and vegetation water content.

## 3. RESULTS AND DISCUSSION

### 3.1. The Effect of Rocks on Brightness Temperature

Due to Eqn. 2, the emission response of rock mixed pixels is combined by the microwave characteristics of the rock component and soil component. The curves of synthetic brightness temperature vary from the brightness temperature curves of soil component to those of rock component as rock cover fraction increases. Fig. 1 illustrates the changes in brightness temperature simulated as a function of bulk soil moisture, incidence angle, and vegetation water content for various rock cover fractions under specific conditions. Similar results can be gained on other short vegetation conditions. In Fig. 1(a), the bulk soil moisture and soil component VWC are fixed at  $0.15 \text{ m}^3/\text{m}^3$  and  $0.5 \text{ kg}/\text{m}^2$  respectively, representing a short grass covered dry soil condition. Clearly, as incidence angle increased, the impact of rock cover fraction to V-polarized brightness temperature decreased. The sensitivity of V-polarized brightness temperature to rock cover fraction reaches a minimum value when the incidence angle is around  $60^\circ$ . Given these results, it may be possible to estimate the rock cover fraction from the multi-incidence angle response, as will be available from SMOS. In Fig. 1(b), the incidence angle is fixed at  $42.5^\circ$ , which is the fixed incidence angle of SMOS L1C browse products (McMullan *et al.*, 2008), and soil component vegetation water content is again fixed at  $0.5 \text{ kg}/\text{m}^2$ . As expected, the sensitivity of brightness temperature simulations to soil moisture decreases with increasing rock cover fraction. Due to Eqn. 1, the range of bulk soil moisture is restricted by the range of soil component moisture  $SM_{soil}$  and rock fraction  $fr$ , thus limiting bulk moisture to less than  $0.6 \times (1 - fr)$  assuming the water content capacity of soil component is at saturation. These results are in agreement with those obtained by Jackson *et al.* (1992) and Monerris *et al.* (2008), who showed that the brightness temperature emissions from soils with higher rock cover fractions become less sensitive to changes in the

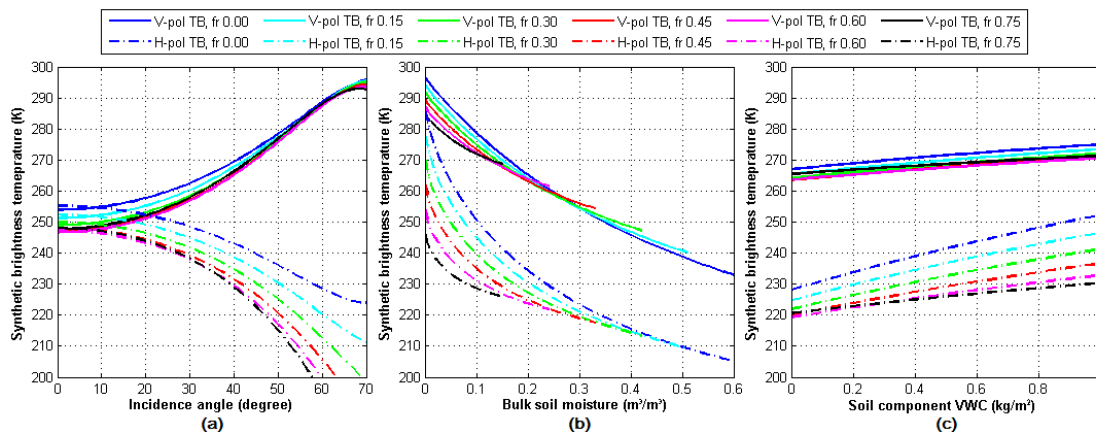


**Figure 1.** Synthetic brightness temperature simulations for varying rock cover fractions as a function of (a) incidence angle; (b) bulk soil moisture; and (c) soil component vegetation water content.

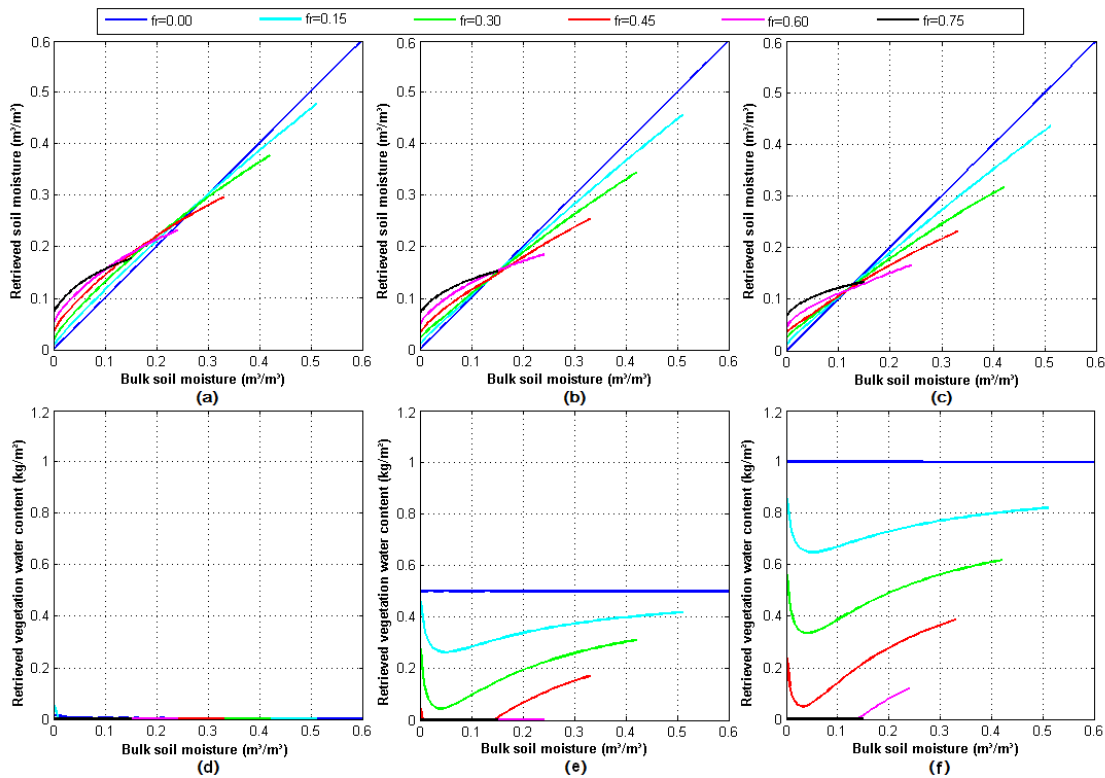


**Figure 2.** Relationship of retrieved soil moisture (top row) and vegetation water content (bottom row) with bulk soil moisture for different rock cover fractions  $f_r$  and vegetation conditions: (a) and (d)  $VWC=0.0 \text{ kg/m}^2$ ; (b) and (e)  $VWC=0.5 \text{ kg/m}^2$ ; (c) and (f)  $VWC=1.0 \text{ kg/m}^2$ .

surface soil moisture content. In Fig. 1(c), the bulk soil moisture and incidence angle are again fixed at  $0.15 \text{ m}^3/\text{m}^3$  and  $42.5^\circ$ , respectively. In addition, Figs. 1(a)-(c) imply that the synthetic brightness temperature in H polarization is more sensitive to rock cover fraction than that in V polarization.

### 3.2. The Effect of Rocks on Soil Moisture Retrieval

Figs. 2(a)-(c) illustrate the relationship between truth soil moisture and retrieved soil moisture across three different vegetation conditions. Soil moisture retrieval error is not only dependent on rock cover fraction but also on bulk soil moisture and vegetation water content. In some bulk soil moisture and vegetation water content conditions, rock cover fraction has little impact on soil moisture retrieval accuracy. For example, in Fig. 2(b), when the bulk soil moisture approaches  $0.15 \text{ m}^3/\text{m}^3$ , retrieved soil moisture is equal to bulk soil moisture in all ranges of rock cover fraction. It can be seen that the soil moisture retrieval model will overestimate the bulk soil moisture in dry conditions and underestimate it in wet conditions if the presence of rock is not accounted for. In the whole range of bulk soil moisture, especially under wet soil conditions, rock induces a soil moisture retrieval error exceeding the  $0.04 \text{ m}^3/\text{m}^3$  error budget of SMOS for most cover fractions. However, a low rock cover fraction in dry soil conditions leads to a retrieval error smaller than  $0.04 \text{ m}^3/\text{m}^3$ . Additionally, the higher the VWC of the soil component, the larger the soil moisture retrieval error incurred. Figs. 2(d)-(f) illustrate the retrieved vegetation water contents concurrent with retrieved soil moisture shown in Fig. 2(a)-(c). The retrieved VWC decreases with increased rock cover fraction for two reasons. First, the rock component in land surface representation was assumed to be vegetation-free in this study. The presence of rock therefore reduces the average VWC over the entire field. Second, the presence of surface rock increases the difference between H and V polarized brightness temperature, thus the optimization scheme in L-MEB decrease the retrieved VWC in order to minimize the cost function since VWC is much more sensitive to the separation than soil moisture. When retrieved VWC reaches 0, it can be no further improvement in  $T_b$ , and a non-convergence flag is returned since the tolerance is not achieved.

### 3.3. General Sensitivity Study

The results presented so far assumed a smooth rock surface unobscured by vegetation, with a constant rock and soil temperature, and a predefined rock dielectric constant. However, the effects of rock on soil moisture

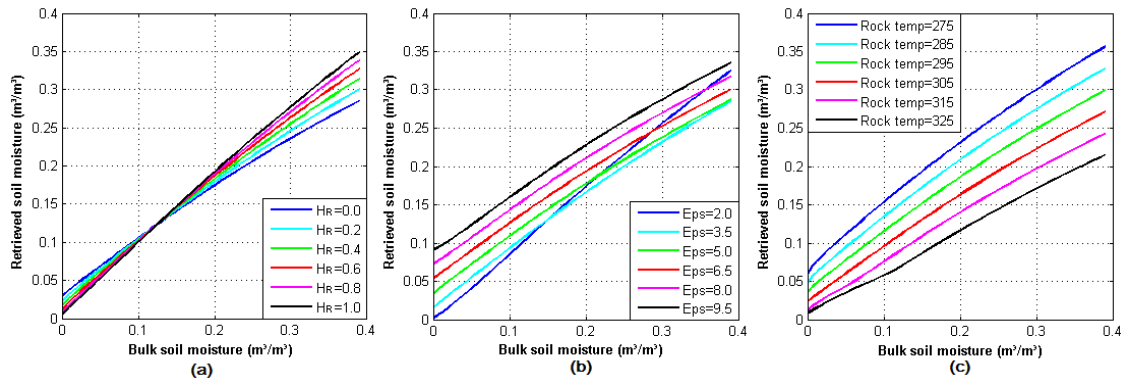


**Figure 3.** Relationship between bulk soil moisture and retrieved soil moisture for different (a) rock surface roughness; (b) rock dielectric constant; and (c) rock temperature.

retrieval accuracy are not only dependent on the rock cover fraction, incidence angle and vegetation water content that were assessed, but also on these other fixed parameters and assumptions. In this section, the sensitivities of the retrieved soil moisture to rock surface roughness, rock temperature and dielectric constant are examined, based on a typical rock cover fraction of 0.35 (Jackson *et al.*, 1992).

Fig. 3 shows the sensitivity of the retrieved soil moisture to changes in the rock surface roughness, effective rock temperature and rock dielectric constant as a function of bulk soil moisture. Clearly, the rock roughness parameter has a significant impact on rock induced soil moisture retrieval error. Since the difference between H and V polarized brightness temperature of smooth rock is much larger than that of soil, the higher the rock surface roughness parameter  $H_R$ , the smaller the difference between the polarization gap of soil and rock components, and the smaller the soil moisture retrieval error due to the presence of rock. Moreover, changes in the real part of the rock dielectric constant and rock temperature are not able to change the pattern in which the rock cover fraction affects the soil moisture retrieval error, but both affect the magnitude of rock induced errors. The rock dielectric constant and rock temperature influence the retrieved soil moisture in different ways; approximately every 1.5 increase of real part of rock dielectric constant leads to  $0.02 \text{ m}^3/\text{m}^3$  increase in retrieved soil moisture, while higher rock temperature corresponds to a soil moisture decrease of  $0.01\text{--}0.02 \text{ m}^3/\text{m}^3$  per 10K increase of rock surface temperature.

#### 4. CONCLUSION

A simple short grass land representation was studied to assess the effect of rock cover fraction on soil moisture retrieval assuming rock behaves like very dry soil with smooth surface and without attenuation by surrounding vegetation. Based on this synthetic study, it was shown that uncertainty in the rock cover fraction results in a significant effect on the retrieval accuracy of soil moisture from remotely sensed brightness temperature observations. For bare soil, maximum error in the bulk soil moisture estimation is as much as  $0.04 \text{ m}^3/\text{m}^3$  and up to  $0.10 \text{ m}^3/\text{m}^3$  in wet soil covered by short grass vegetation ( $\text{VWC} = 1 \text{ kg}/\text{m}^2$ ) for 30% rock cover fraction. It was also shown that the omission of rock cover from the retrieval algorithm leads to an overestimation of the bulk soil moisture content for low soil moisture conditions and an underestimation for high soil moisture conditions. Rock surface roughness, rock temperature and rock dielectric constant were found to have a significant impact on the retrieval of soil moisture; a fact that has largely been ignored in the past and should be studied further.

While it may seem at first difficult to apply the findings presented here to practical applications, due to the lack of sufficient data on global rock cover fraction, it is suggested that the relationships shown in this study may be exploited to determine the rock cover fraction for individual footprints by using the multi-angular data that will be provided by SMOS. As the rock fraction and its dielectric constant are constant through time, it may be possible to estimate the rock cover fraction from multi-angular data.

#### ACKNOWLEDGMENTS

This project is funded by an Australian Research Council Discovery Project (DP0879212). Ye Nan is sponsored by a Melbourne International Fee Remission Scholarship (MIFRS). The authors wish to thank Jean-Pierre Wigneron for providing the source code of L-MEB.

## REFERENCES

- Delwart, S., Bouzinac, C., Wursteisen, P., Berger, M., Drinkwater, M., Martín-Neira, M., and Kerr, Y.H. (2008), SMOS validation and the COSMOS campaigns. *IEEE Transactions on Geoscience and Remote Sensing*, 46(3), 695–704.
- Dobson, M.C., Ulaby, F.T., Hallikainen, M.T., and El-Rayes, M.A. (1985), Microwave dielectric behaviour of wet soil—part II: Dielectric mixing models. *IEEE Transactions on Geoscience and Remote Sensing*, GE-23(1), 35–46.
- Jackson, T.J., Kostov, K.G., and Saatchi, S.S. (1992), Rock fraction effects on the interpretation of microwave emission from soils. *IEEE Transactions on Geoscience and Remote Sensing*, 30(3), 610–616.
- Jackson, T.J. and Schmugge, T.J. (1989), Passive microwave remote sensing system for soil moisture: Some supporting research. *IEEE Transactions on Geoscience and Remote Sensing*, 27, 225–235.
- Kerr, Y.H., Waldteufel, P., Richaume, P., Davenport, I., Ferrazzoli, P., and Wigneron, J.-P. (2007), SMOS level 2 processor soil moisture algorithm theoretical basis document (ATBD). *CESBIO, Toulouse, France. SM-ESL (CBSA), SO-TN-ESL-SM-GS-0001*, ESA Internal report, V2.a. [Online]. Available: <http://www.cesbio.ups-tlse.fr/us/indexsmos.html>.
- Kerr, Y.H., Waldteufel, P., Wigneron, J.-P., Font, J., and Berger, M. (2003), The Soil moisture and ocean salinity mission. *IEEE, General Presentation*.
- McMullan, K.D., Brown, M.A., Martín-Neira, M., Rits, W., Ekholm, S., Marti, J., and Lemanczyk, J. (2008), SMOS: The Payload. *IEEE Transactions on Geoscience and Remote Sensing*, 46(3), 594–605.
- Mo, T., Choudhury, B.J., Schmugge, T.J., Wang, J.R., and Jacscon, T.J. (1982), A model for the microwave emission of vegetation-covered fields. *Journal of Geophysical Research*, 87(11), 229–237.
- Moneris, A., Vall-llossera, M., Camps, A., and Piles, M. (2008), Rock fraction effects on the surface soil moisture estimates from L-band radiometric measurement. *IEEE IGARSS*, 2008, 711–714.
- Njoku, E.G., Wilson, W.J., Yueh, S.H., Dinardo, S.J., Li, F.K., Jackson, T.J., Lakshmi, V., and Bolten, J. (2002), Observations of soil moisture using a passive and active low-frequency microwave airborne sensor during SGP99. *IEEE Transactions on Geoscience and Remote Sensing*, 40(12), 2659–2673.
- Owe, M., de Jeu, R., and Holmes, T. (2008), Multisensor historical climatology of satellite-derived global land surface moisture, *Journal of Geophysics Research*, 113, F01002.
- Panciera, R., Walker, J.P., Kalma, J.D., Kim, E.J., Saleh, K., and Wigneron J.-P. (2009), Evaluation of the SMOS L-MEB passive microwave soil moisture retrieval algorithm. *Remote Sensing of Environment*, 113, 435–444.
- Rüdiger, C., Calvet, J.-C., Gruhier, C., Holmes, T., de Jeu, R., and Wagner, W. (2009), An Intercomparison of ERS-Scat and AMSRE Soil Moisture Observations with Model Simulations over France. *Journal of Hydrometeorology*, in press, doi:10.1175/2008JHM997.1.
- Wang, J.R. and Choudhury, B.J. (1981), Remote sensing of soil moisture content over bare field at 1.4 GHz frequency. *Journal of Geophysical Research*, 86, 5277–5282.
- Wigneron, J.-P., Laguerre, L., and Kerr, Y. (2001), Simple modeling of the L-band microwave emission from rough agricultural soils. *IEEE Transactions on Geoscience and Remote Sensing*, 39(8), 1697–1707.
- Wigneron, J.-P., Kerr, Y., Waldteufel, P., Saleh, K., Escorihuela, M.-J., Richaume, P., Ferrazzoli, P., de Rosnay, P., Gurney, R., Calvet, J.-C., Grant, J.P., Guglielmetti, M., Hornbuckle, B., Mätzler, C., Pellarin T., and Schwank, M. (2007), L-band Microwave Emission of the Biosphere (L-MEB) model: Description and calibration against experimental data sets over crop fields. *Remote Sensing of Environment*, 107, 639–655.
- Ulaby, F.T., Bengal, T.H., Dobson, M.C., East, J.R., Garvin, J.B., and Evans, D.L. (1990), Microwave Dielectric Properties of Dry Rocks. *IEEE Transactions on Geoscience and Remote Sensing*, 28(3), 325–336.
- Ulaby, F.T., Moore, R.K., and Fung, A.K. (1986), *Microwave Remote Sensing: Active and Passive*. vol. 3. Norwood, USA: Artech House.